

Renormalization group method for weakly-coupled quantum chains: application to the spin one-half Heisenberg model

S. Moukouri

*Michigan Center for Theoretical Physics and Department of Physics,
University of Michigan 2477 Randall Laboratory, Ann Arbor MI 48109*

The Kato-Bloch perturbation formalism is used to present a density-matrix renormalization-group (DMRG) method for strongly anisotropic two-dimensional systems. This method is used to study Heisenberg chains weakly coupled by the transverse couplings J_{\perp} and J_d (along the diagonals). An extensive comparison of the renormalization group and quantum Monte Carlo results for parameters where the simulations by the latter method are possible shows a very good agreement between the two methods. It is found, by analyzing ground state energies and spin-spin correlation functions, that there is a transition between two ordered magnetic states. When $J_d/J_{\perp} \lesssim 0.5$, the ground state displays a Néel order. When $J_d/J_{\perp} \gtrsim 0.5$, a collinear magnetic ground state in which interchain spin correlations are ferromagnetic becomes stable. In the vicinity of the transition point, $J_d/J_{\perp} \approx 0.5$, the ground state is disordered. But, the nature of this disordered ground state is unclear. While the numerical data seem to show that the chains are disconnected, the possibility of a genuine disordered two-dimensional state, hidden by finite size effects, cannot be excluded.

I. INTRODUCTION

In a recent publication¹, it was shown that the density-matrix renormalization group method (DMRG)^{2,3} can be applied to an array of weakly coupled quantum chains. As an illustration of the method, weakly coupled Heisenberg spin chains were studied and some partial results on the ground state energies were shown to be in good agreement with previous quantum Monte Carlo (QMC) studies. But the essential question concerning the stability of the disordered one-dimensional (1D) ground state against small transverse perturbations was not addressed.

The motivation behind such a study is in the search of a disordered ground state for a spin one-half Heisenberg model in dimension higher than one. A spin liquid state without spin rotational or translational symmetry breaking has been conjectured to be relevant for the physics of high-Tc cuprate superconductors⁴. A possible candidate is the resonance valence bond (RVB) state⁵. Earlier attempts^{6,7,8,9} to find the RVB ground state by various techniques (1/S expansions, exact diagonalization, quantum Monte Carlo) have given some indication about its possible realization. But their conclusions are still disputed. It has even been argued¹⁰ that the spin-Peierls mechanism, not RVB, may be the most natural way to lead to a disordered state.

More recently, the interest has shifted to search for a RVB state on quasi 1D systems. A pure spin one-half Heisenberg chain has a disordered ground state with neutral spin one-half excitations (spinons) and does not break spin rotational or translational symmetry. It is thus tempting to try to find a higher dimensional generalization of this state by the application of small perturbations. Contrary to an earlier claim of the realization of a spin liquid¹¹, subsequent studies^{12,13,14} indicate that the introduction of the rung transverse coupling J_{\perp} between the chains (see Fig. 1) seems to lead to a Néel state for any non-zero J_{\perp} . A possible way to avoid the Néel or-

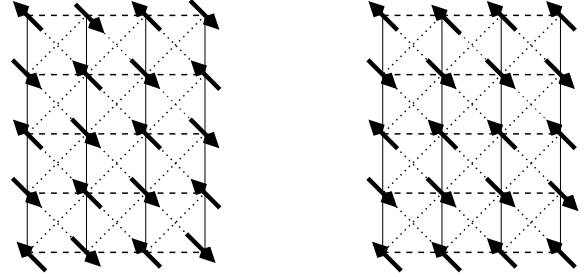


FIG. 1: Sketch of the ground state of weakly coupled Heisenberg chains as function of J_{\perp} (dashed lines along the rungs) and J_d (dotted lines along the diagonals): Néel state when $J_d/J_{\perp} \lesssim 0.5$ (left), collinear state when $J_d/J_{\perp} \gtrsim 0.5$ (right)

der is to introduce, in addition to J_{\perp} , a small frustration J_d along the diagonals. In a recent work¹⁵ it was claimed that a spin liquid state is realized when $J_{\perp} = 2J_d$.

A more direct motivation in studying a model of weakly coupled Heisenberg chains stems to its relevance to the understanding of interchain effects in quasi-one-dimensional materials^{16,17,18}. A recent neutron scattering experiment¹⁹ on the frustrated antiferromagnet (AFM) Cs_2CuCl_4 found that the dynamical correlation show a highly dispersive continuum of a excitations with fractional quantum numbers, a signature of a spin liquid state.

In this paper, a general formalism of the DMRG algorithm for weakly coupled chains of Ref.¹ is presented. This method is a particular case of a recent matrix version²⁰ of the general perturbation expansion which was proposed decades ago by Kato and Bloch^{21,22,23}. The Kato-Bloch expansion was initially introduced to find the correction on a single state. This expansion is straightforwardly generalized to account for many low lying states. The method is in spirit close to an earlier perturbative renormalization group by Hirsch and Mazenko²⁴. A more detailed study of weakly coupled

Heisenberg chains is presented. An extensive comparison with quantum Monte Carlo results for unfrustrated transverse couplings is made. It shows a good agreement between the two methods when the perturbation is small and the lattice not too large. Then the question of the stability of the non-magnetic state in the presence of frustration is addressed. It is shown that the 2D DMRG algorithm can provide a convincing answer to this question, at least for the parameters that were investigated. It is found, by analyzing ground state energies and spin-spin correlation functions, that the perturbation is relevant, leading to magnetic ground states (see Fig. 1). When $J_d/J_\perp \lesssim 0.5$, the ground state displays a Néel order. When $J_d/J_\perp \gtrsim 0.5$ a collinear magnetic ground state in which interchain spin correlations are ferromagnetic becomes stable. In the vicinity of the transition point, $J_d/J_\perp \approx 0.5$, the system seems to behave as an assembly of independent chains. This is reminiscent of the so-called sliding Luttinger liquid²⁶ recently found in a model of crossed spin one-half Heisenberg chains²⁵. But it is impossible to exclude a genuine 2D spin liquid state (i.e., with a spin gap) masked by finite size effects.

II. FORMAL DEVELOPMENT

The DMRG method described below can work for spin, fermionic as well as bosonic systems, and so it is convenient to use a general formulation of the algorithm that can then be adapted to each of these cases. The model Hamiltonians under consideration can be written as follows:

$$H = H_\parallel + gH_\perp, \quad (1)$$

where H_\parallel is the sum over one-dimensional (1D) Hamiltonians (longitudinal direction),

$$H_\parallel = \sum_{l=1}^L H_l, \quad (2)$$

and H_\perp is the interaction between these 1D systems (transverse direction). The coupling constant g is such that $g \ll 1$.

Since $g \ll 1$, it is natural to study the problem using perturbation theory. The Kato-Bloch formalism is convenient to set up a perturbation expansion around a numerical solution of H_\parallel provided by the DMRG. For a single chain l whose Hamiltonian is H_l , a set of eigenstates $|\phi_{n_l}\rangle$ and eigenvalues ϵ_{n_l} can be obtained by the usual 1D DMRG. The zeroth order set of eigenstates $|\Phi_{\parallel[n]}\rangle$ of the full longitudinal Hamiltonian is simply given by the tensor product of the $|\phi_{n_l}\rangle$,

$$|\Phi_{\parallel[n]}\rangle = |\phi_{n_1}\rangle|\phi_{n_2}\rangle\cdots|\phi_{n_L}\rangle, \quad (3)$$

and the set of approximate eigenvalues of H_\parallel is given by the sum

$$E_{\parallel[n]} = \epsilon_{n_1} + \epsilon_{n_2} + \cdots + \epsilon_{n_L}, \quad (4)$$

where $[n] = (n_1, n_2, \dots, n_L)$ and n_l labels to an eigenset on the chain l .

Let P_\parallel be the projector on the states $|\Phi_{\parallel[n]}\rangle$,

$$P_\parallel = \sum_{[n]} |\Phi_{\parallel[n]}\rangle\langle\Phi_{\parallel[n]}| \quad (5)$$

and $Q_\parallel = 1 - P_\parallel$.

Let $(E_{[n]}, |\Phi_{[n]}\rangle)$ be the exact eigenset of H . This eigenset will tend to $(E_{\parallel[n]}, |\Phi_{\parallel[n]}\rangle)$ in the limit $g \rightarrow 0$. Let P be the projector onto the spaces $|\Phi_{[n]}\rangle$. P may be written as follows

$$P = \sum_{[n]} |\Phi_{[n]}\rangle\langle\Phi_{[n]}|. \quad (6)$$

Since the perturbation g is small, it is assumed that the subspaces generated by the $|\Phi_{\parallel[n]}\rangle$'s and by the $|\Phi_{[n]}\rangle$'s are not orthogonal. An approximate expression of HP in the basis spanned by the eigenstates of H_\parallel will now be derived by using a generalization of a method first introduced by Kato²¹ and later modified by Bloch²². The advantage of the Bloch's version is that it leads to a simpler expansion.

Following Bloch, let \mathcal{U} be the operator

$$\mathcal{U} = \sum_{[n]} |\Phi_{[n]}\rangle\langle\Phi_{\parallel[n]}| \quad (7)$$

which projects the $|\Phi_{\parallel[n]}\rangle$ onto $|\Phi_{[n]}\rangle$, and \mathcal{U} satisfies, $\mathcal{U}P_\parallel = \mathcal{U}$. The problem of finding an expansion of HP projected onto P_\parallel is equivalent to finding an expansion for $P_\parallel H \mathcal{U}$.

One starts by deriving an equation satisfied by \mathcal{U} . The Schrödinger equation

$$H|\Phi_{[n]}\rangle = E_{[n]}|\Phi_{[n]}\rangle \quad (8)$$

is transformed as follows,

$$(H - \tilde{H}_\parallel)|\Phi_{[n]}\rangle = \mathcal{E}_{[n]}|\Phi_{[n]}\rangle \quad (9)$$

where \tilde{H}_\parallel is identical to H_\parallel in the subspace spanned by the $|\Phi_{\parallel[n]}\rangle$'s, and,

$$\mathcal{E}_{[n]} = E_{[n]} - \langle\Phi_{[n]}|\tilde{H}_\parallel|\Phi_{[n]}\rangle. \quad (10)$$

When a single state $|\Phi_{\parallel[0]}\rangle$ is kept, \tilde{H}_\parallel is given by

$$\tilde{H}_{\parallel} = \begin{pmatrix} E_{\parallel[0]} & 0 & 0 & 0 & 0 & \dots & 0 \\ 0 & E_{\parallel[0]} & 0 & 0 & 0 & \dots & 0 \\ 0 & 0 & E_{\parallel[0]} & 0 & 0 & \dots & 0 \\ & & \dots & & & \dots & \\ 0 & 0 & \dots & E_{\parallel[0]} & \dots & \dots & \\ 0 & 0 & 0 & \dots & E_{\parallel[0]} & \dots & 0 \\ & & \dots & & & \dots & \\ 0 & 0 & 0 & 0 & 0 & \dots & E_{\parallel[0]} \end{pmatrix}.$$

The method reduces to the usual stationary perturbation expansion. It is known that such an expansion does not often converge. The main source of divergence is the near degeneracy of the eigenvalues. Now if many states up to a cut-off n_c are kept, a possible generalization of \tilde{H}_{\parallel} to many states $|\Phi_{\parallel[0]}\rangle > \dots |\Phi_{\parallel[n_c]}\rangle$, is

$$\bar{H}_{\parallel} = \begin{pmatrix} E_{\parallel[0]} & 0 & 0 & 0 & 0 & \dots & 0 \\ 0 & E_{\parallel[1]} & 0 & 0 & 0 & \dots & 0 \\ 0 & 0 & E_{\parallel[2]} & 0 & 0 & \dots & 0 \\ & & \dots & & & \dots & \\ 0 & 0 & \dots & E_{\parallel[n_c]} & \dots & \dots & \\ 0 & 0 & 0 & \dots & E_{\parallel[0]} & \dots & 0 \\ & & \dots & & & \dots & \\ 0 & 0 & 0 & 0 & 0 & \dots & E_{\parallel[0]} \end{pmatrix}.$$

Thus if n_c is suitably chosen, the series will converge²⁰. The purpose of this choice is to shield the eigenvalue $E_{\parallel[0]}$ from the rest of the spectrum by treating the $n_c - 1$ states just above the ground state exactly and the remaining spectrum perturbatively.

By applying P_{\parallel} and then \mathcal{U} to the Equation(9) above, one finds,

$$g\mathcal{U}H_{\perp}|\Phi_{[n]}\rangle = \mathcal{E}_{[n]}|\Phi_{[n]}\rangle \quad (11)$$

The subtraction of Equation(11) from Equation(9) leads to

$$(H - \tilde{H}_{\parallel} - g\mathcal{U}H_{\perp})|\Phi_{[n]}\rangle = 0. \quad (12)$$

By applying $\langle\Phi_{\parallel[n]}|$ on the right of equation(12) and performing the summation over $[n]$, one finally obtains the equation satisfied by \mathcal{U} ,

$$(H - \tilde{H}_{\parallel} - g\mathcal{U}H_{\perp})\mathcal{U} = 0. \quad (13)$$

Equation(13) is further transformed by using the fact that $P_{\parallel}\mathcal{U} = P_{\parallel}$ and $\mathcal{U} = P_{\parallel}\mathcal{U} + Q_{\parallel}\mathcal{U}$. One obtains:

$$\mathcal{U} = P_{\parallel} + g\tilde{Q}_{\parallel}(H_{\perp}\mathcal{U} - \mathcal{U}H_{\perp}\mathcal{U}) \quad (14)$$

where \tilde{Q}_{\parallel} is given by

$$\tilde{Q}_{\parallel} = Q_{\parallel}(\tilde{H}_{\parallel} - H_{\parallel})^{-1}. \quad (15)$$

This leads to the expansion for \mathcal{U}

$$\mathcal{U}^{(0)} = P_{\parallel} \quad (16)$$

$$\mathcal{U}^{(n)} = g\tilde{Q}_{\parallel}[H_{\perp}\mathcal{U}^{(n-1)} - \sum_{p=1}^{n-1}\mathcal{U}^{(p)}H_{\perp}\mathcal{U}^{(n-p-1)}] \quad (17)$$

From this expansion, one finds the approximate Hamiltonian $\tilde{H} = P_{\parallel}H\mathcal{U}$ is

$$\begin{aligned} \tilde{H} = \sum_{[n]} E_{\parallel[n]}|\Phi_{\parallel[n]}\rangle\langle\Phi_{\parallel[n]}| + gP_{\parallel}H_{\perp}P_{\parallel} + \\ g^2P_{\parallel}H_{\perp}\tilde{Q}_{\parallel}H_{\perp}P_{\parallel} + \dots \end{aligned} \quad (18)$$

This perturbation expansion is a matrix generalization to many states of Bloch's expansion^{22,23} which was established for a single state. Even though the ground state and a few low lying states will ultimately be computed, it is important to keep many low lying states in the perturbation expansion. This is because the convergence will mainly depend on two quantities. The first one is obviously g . The second one is the projector \tilde{Q}_{\parallel} . If $\tilde{H}_{\parallel} = H_{\parallel}$, then $\tilde{Q}_{\parallel} = 0$. In that case only the first order term in equation (18) is not equal to zero. The rewriting of the original problem to equation (18) is a simple change of basis. So in the limit where $n_c = \dim A$, where A is the Hilbert space in which all the operators are defined, the method is exact. But since only a small number of eigenstates of H_{\parallel} can be used even if the full spectrum is known, $\tilde{Q}_{\parallel} \neq 0$. The magnitude of \tilde{Q}_{\parallel} in the expansion decreases by increasing the cut-off n_c . It is to be noted this matrix expansion is close to the method of Hirsch and Mazenko²⁴, who also used a block expansion near the solution of an unperturbed Hamiltonian. The problem with their study was, however, that their technique was applied to a model with no small parameter.

When the DMRG is used as a method of solution for H_{\parallel} , we can not know Q_{\parallel} exactly. This is because the DMRG does not keep any information about the truncated states. But it is possible to define a perturbative expansion in a reduced space spanned by the states kept. The above perturbative expansion will thus be adapted in this study as follows. During the 1D DMRG part of the method, $N_s = ms_1 \times ms_1$ states will be obtained for the reduced superblock (i.e., the superblock reduced to the two external large blocks; it is supposed that open boundary conditions (OBC) are used). Typically $ms_1 = 16 - 192$ during this investigation. The complete spectrum of this reduced superblock can be obtained as in the thermodynamic algorithm²⁷. This spectrum will serve as H_{\parallel} . Only a small fraction $ms_2 = 16 - 96$ of these states can be kept for the generation of the 2D lattice. The ms_2 states will define P_{\parallel} , and Q_{\parallel} is constructed using the remaining $N_s - ms_2$ states. Hence the perturbation expansion in Eq.(18) will be made by

assuming that H_{\parallel} is the low energy Hamiltonian of size $ms_1 \times ms_1$ obtained from the DMRG rather than the exact 1D solution of H_{\parallel} .

The Hamiltonian \tilde{H} is one-dimensional and it will be studied by the DMRG method. The only difference with a normal 1D situation is that the local operators are now $ms_2 \times ms_2$ matrices which makes computations heavier. It should be noted that the accuracy of the method is related to the diagonalized unperturbed Hamiltonian obtained from the DMRG. This Hamiltonian, although it leads to a very accurate ground state energy, is less accurate for high lying states and correlation functions. So the potential errors of the method will come from the DMRG as well as the truncated perturbative series. A better approach is to use the exact diagonalization method to diagonalize the unperturbed Hamiltonian. However, in that case one will be restricted to small chains.

III. APPLICATION TO THE HEISENBERG MODEL

The above formalism will now be applied to the anisotropic Heisenberg model on a 2D square lattice. The Hamiltonian reads:

$$H_{spins} = \sum_{i,l} \mathbf{S}_{i,l} \mathbf{S}_{i+1,l} + J_{\perp} \sum_{i,l} \mathbf{S}_{i,l} \mathbf{S}_{i,l+1} + J_d \sum_{i,l} (\mathbf{S}_{i,l} \mathbf{S}_{i+1,l+1} + \mathbf{S}_{i+1,l} \mathbf{S}_{i,l+1}) \quad (19)$$

where the $\mathbf{S}_{i,l}$ are the usual spin one-half operators.

The question of the condition of the onset of long-range order as a function of J_{\perp} has been addressed in many studies. Spin-wave analysis^{11,28} predicted that there is a finite critical $J_{\perp c} \approx 0.03$, above which long-range order is established. Renormalization group analysis¹² supplemented by series expansion computations found that if $J_{\perp c}$ is finite, it cannot exceeds 0.02. A finite critical value is at variance with a random phase approximation

(RPA)¹³ which predicts $J_{\perp c} = 0$. The QMC method combined with a multichain mean-field approach¹⁴ has concluded that when $J_{\perp} = 0$, the ground state is an anti-ferromagnet down to $J_{\perp} = 0.02$. From these studies, it is likely that the AFM ground state is stable as soon as $J_{\perp} \neq 0$. This does not, however, preclude a spin liquid ground state in the case when J_d is added between the chains. When this exchange term is added, the QMC method faces the infamous sign problem. The two-step DMRG method presented here can help to find, if it exists, the spin liquid ground state.

The adaptation of the formalism discussed in section(II) to the model of Equation(19) is without any difficulty. The first step is the solution of the 1D Hamiltonian:

$$H_l = \sum_i \mathbf{S}_{i,l} \mathbf{S}_{i+1,l} \quad (20)$$

by the usual DMRG method. This yields the chain eigenvalues ϵ_{n_l} and eigenstates $|\phi_{n_l}\rangle$. From equation (18), the projected Hamiltonian in the first order approximation is given by

$$\tilde{H} = \sum_{[n]} E_{\parallel[n]} |\Phi_{\parallel[n]}\rangle \langle \Phi_{\parallel[n]}| + J_{\perp} P_{\parallel} \sum_{i,l} \mathbf{S}_{i,l} \mathbf{S}_{i,l+1} P_{\parallel} + J_d P_{\parallel} \sum_{i,l} (\mathbf{S}_{i,l} \mathbf{S}_{i+1,l+1} + \mathbf{S}_{i+1,l} \mathbf{S}_{i,l+1}) P_{\parallel} \quad (21)$$

which may simply be written as

$$\tilde{H} \approx \sum_{[n]} E_{\parallel[n]} |\Phi_{\parallel[n]}\rangle \langle \Phi_{\parallel[n]}| + J_{\perp} \sum_{il} \tilde{\mathbf{S}}_{i,l} \tilde{\mathbf{S}}_{i,l+1} + J_d \sum_{il} (\tilde{\mathbf{S}}_{i,l} \tilde{\mathbf{S}}_{i+1,l+1} + \tilde{\mathbf{S}}_{i+1,l} \tilde{\mathbf{S}}_{i,l+1}), \quad (22)$$

where $\tilde{\mathbf{S}}_{i,l}^{n_l, m_l} = \langle \phi_{n_l} | \mathbf{S}_{i,l} | \phi_{m_l} \rangle$.

The matrix elements for the second terms may be written

$$\langle \Phi_{\parallel[n]} | H_{\perp} \tilde{Q}_{\parallel} H_{\perp} | \Phi_{\parallel[n']}\rangle = \sum_{il, i'l', [m]} \frac{\langle \Phi_{\parallel[n]} | \mathbf{S}_{i,l} \mathbf{S}_{i,l+1} | \Phi_{\parallel[m]}\rangle \langle \Phi_{\parallel[m]} | \mathbf{S}_{i',l'} \mathbf{S}_{i',l'+1} | \Phi_{\parallel[n']}\rangle}{E_{\parallel[0]} - E_{\parallel[m]}} \quad (23)$$

The second order term (23) generates a long-range coupling between the chains, which makes it difficult to treat. One can see that the condition for the matrix ele-

ment to be non zero is that $\langle \phi_{n_{l1}} | \phi_{m_{l2}} \rangle = \delta_{n_{l1}, m_{l2}}$ except when $l_{1,2} = l$ or $l+1$. Thus,

$$E_{[m]} - E_{[0]} = (\epsilon_{n_1} - \epsilon_{0_1}) + \dots + (\epsilon_{m_l} - \epsilon_{0_l}) + (\epsilon_{m_{l+1}} - \epsilon_{0_{l+1}}) + \dots + (\epsilon_{n_L} - \epsilon_{0_L}). \quad (24)$$

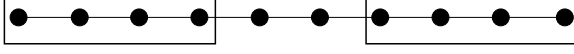


FIG. 2: sketch of the superblock in the step 1

In the Eq. 24 above, the dominant terms will come from the differences involving the indices m_l and m_{l+1} because the others terms come from the state used to generate P_{\parallel} and are thus of lower energies. Up to the second order, the effective one-dimensional Hamiltonian, which is written here without the frustration term, is

$$\tilde{H} \approx \sum_{[n]} E_{\parallel[n]} |\Phi_{\parallel[n]}\rangle \langle \Phi_{\parallel[n]}| + J_{\perp} \sum_l \tilde{\mathbf{S}}_l \tilde{\mathbf{S}}_{l+1} - \frac{J_{\perp}^2}{2} \sum_l \mathbf{S}_l^{(2)} \mathbf{S}_{l+1}^{(2)} + \dots \quad (25)$$

where the chain-spin operators on the chain l are $\tilde{\mathbf{S}}_l = (\tilde{\mathbf{S}}_{1l}, \tilde{\mathbf{S}}_{2l}, \dots, \tilde{\mathbf{S}}_{Ll})$ and $\mathbf{S}_{il}^{(2)} = (\tilde{\mathbf{S}}_{1l}^{(2)}, \tilde{\mathbf{S}}_{2l}^{(2)}, \dots, \tilde{\mathbf{S}}_{Ll}^{(2)})$, L is the chain length. The matrix elements of the second order local spin operators are

$$\mathbf{S}_{il}^{(2)n_l n'_l} = \sum_{m_l} \frac{\tilde{S}_{il}^{n_l m_l} \tilde{S}_{il}^{m_l n'_l}}{\sqrt{\epsilon_{m_l} - \epsilon_{0_l}}}. \quad (26)$$

One can note that this expression of $\mathbf{S}_{il}^{(2)}$ is not exact, it has been simplified to avoid long-range coupling between the chains. The effective 1D Hamiltonian \tilde{H} is also studied using DMRG.

IV. ALGORITHMIC DETAILS

The algorithm of the method will now be described below. It consists of two DMRG steps separated by an intermediate stage in which a simple block decimation is made.

A. Step 1

The first step of the method is the usual DMRG method for a single chain. The chain is divided into four blocks, and the two internal blocks are made of a single site each. In the calculations, $ms_1 = 16 - 192$ states are kept in the two external blocks. In most cases, the initial iteration starts with a chain having the largest size before truncation, for instance $L = 16$ when $ms_1 = 128$ states are kept. This way, a high accuracy is obtained

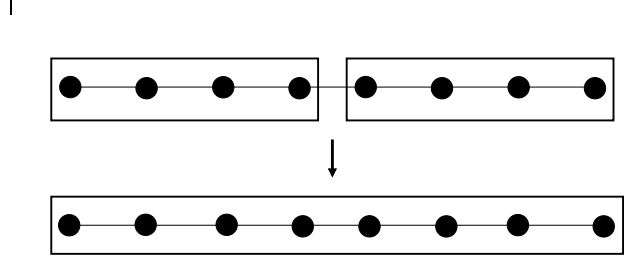


FIG. 3: sketch of the transformation of the two external blocks of length $L/2$ into a single block of length L which is used as the building unit in step 2

even when the infinite system method is used. During this step, the local spin operators \mathbf{S}_i on each site i of the chain are stored and longitudinal spin-spin correlations $C(i, r) = \langle \mathbf{S}_i \mathbf{S}_{i+r} \rangle$ are also computed and stored. As discussed by Caron and Bourbonnais²⁹, open boundary conditions (OBC) which are used here introduce spurious behavior at the edges of the chain. It is therefore better to chose the origin i in $C(i, r)$ in the middle of chain. It is crucial during this step to target more just than the $S_z = 0$ sector in order to obtain a correct low-energy Hamiltonian. In addition to $S_z = 0$, $S_z = \pm 1, \pm 2$ were targeted in this study.

B. Block transformation

An intermediate stage of the algorithm is a decimation process as in the old block renormalization group method^{31,32}. In this process, the two external blocks having $L/2$ sites each are reduced to a single block with L sites. During this step, the $ms_1 \times ms_1$ states describing the chain are reduced to ms_2 lowest states of the chain. As noted in Ref.¹, since the block transformation is used only one time, the problem of the propagation of spurious boundary effects³⁰ is not present. All the local spin operators and spin-spin correlation functions are expressed in the basis of the ms_2 states.

C. Step 2

The second step consists of applying the 1D DMRG method using the chains obtained at the end of the previous step as the building blocks. This step is indeed identical to the first step, except for the dimension of the local spin operators. The central block is the chain from the previous step and thus has the dimension $ms_2 \times ms_2$. Typically, $ms_2 = 16 - 96$ and for the two external blocks, roughly the same number of states is kept. If four blocks were taken as in the first step, the dimension of the su-

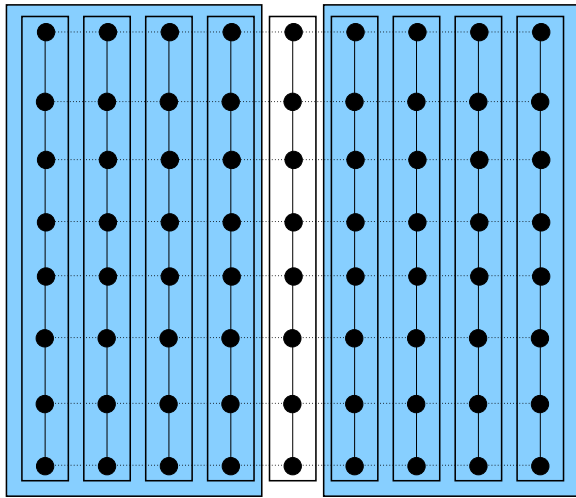


FIG. 4: Sketch of the superblock in step 2

perblock would be ms_2^4 which can become rapidly impractical. To ease the computations, three blocks instead of four are mostly used during this step. As will be seen below, it is important during this step to check that, for a given value of the couplings J_\perp and J_d , enough states are kept such that a valid computation is made. i.e., that the truncated Hamiltonian generated for the single chain is accurate enough, for the ground state and for the low lying states, to be used as a building block for the 2D lattice. One can easily see that for a fixed L and $J_{\perp,d} \ll \Delta_\sigma(L)$, $\Delta_\sigma(L)$ is the finite size spin gap, and the interchain matrix elements will be negligible. The system will behave as a collection of free chains even if $J_{\perp,d}$ is turned on. Now if $J_{\perp,d} \sim \delta E(L)$, where $\delta E(L)$ is the width of the retained states, the matrix elements of the states having higher energy, which have been truncated out, have a non-negligible contribution.

D. Algorithm

The algorithm is summarized below.

- 1. Build the low energy Hamiltonian for a single chain $B \cdot \cdot B$ by using the 1D DMRG algorithm of Ref². Store the spin operator \mathbf{S}_i on each site and the correlation function $C(i, r)$.
- 2. When the block B size is $L/2$, apply the block method to merge the two external blocks into a single block defined by the ms_2 states kept. Express all the spin operators and correlation functions in the basis of the ms_2 states. Check if for the number of states kept, the transverse couplings satisfy $\Delta_\sigma(L) \lesssim J_{\perp,d} \ll \delta E(L)$. If this condition is not satisfied, increase ms_2 .
- 3. Start a second 1D DMRG simulation identical to the first one except that the central block is now

J_\perp	$ms_2 = 16$	$ms_2 = 24$	$ms_2 = 32$	QMC
0.00	-0.42848	-0.42851	-0.42851	-0.42849(2)
0.05	-0.42900	-0.42907	-0.42909	-0.42926(2)
0.10	-0.43058	-0.43078	-0.43090	-0.43147(2)
0.15	-0.43312	-0.43361	-0.43387	-0.43530(2)
0.20	-0.43642	-0.44733	-0.43780	-0.44064(2)
0.25	-0.44028	-0.44174	-0.44247	-0.44727(2)

TABLE I: DMRG ground state energies for 12×12 lattices for $ms_1 = ms_2 = 16, 24$, and 32 versus QMC.

a single chain instead of a site, and the exchange coupling is $J_{\perp,d}$ instead of 1.0.

V. RESULTS WITH FOUR BLOCKS IN STEP 2

In this part, the DMRG results are compared to the stochastic series expansion (SSE) QMC results. The SSE-QMC method³³ is so far the most reliable technique for the study of quantum spin systems. It has been used to study weakly coupled quantum spin chains¹⁴. It will thus be very instructive to see how well the DMRG method compares to the SSE-QMC.

A. First order ground-state energies

In Table (I), the ground state energy per site for 12×12 systems for $m = 16, 24$ and 32 is shown. In this calculation, four blocks were used in the second DMRG step. The agreement with the SSE-QMC results is good for small g . The DMRG energies are higher than those of the QMC for all transverse couplings studied. As ms_2 is increased, the difference between the DMRG and QMC energies decreases. This was expected since the current method as the original DMRG procedure is variational.

The band-width of the states kept is $\Delta E = 1.132, 1.290, 1.466$ when $ms_2 = 16, 24$ and 32 respectively. The target states during the first DMRG step were the lowest states of the spin sectors with $S_z = 0, \pm 1 \pm 2$. The lowest states of higher spin sectors have energies which are higher than the highest state kept in lower spin sectors, therefore they were not targeted. The fact that the DMRG results compare well with the QMC ones even at intermediate couplings reveals that for the spin chain, reliable calculations can be made for values of $\delta E(L)/J_\perp \approx 5$. But as expected for higher values of J_\perp , the condition $\delta E(L)/J_\perp \gg 1$ is no longer fulfilled. This means the Hilbert space is too severely truncated.

B. Second order ground-state energies

Table II displays second order ground-state energies for a 12×12 system which are compared with QMC. The agreement is systematically better than in the first order

J_{\perp}	$ms_2 = 16$	$ms_2 = 24$	$ms_2 = 32$	QMC
0.00	-0.42848	-0.42851	-0.42851	-0.42849(2)
0.05	-0.42901	-0.42909	-0.42910	-0.42926(2)
0.10	-0.43063	-0.43083	-0.43094	-0.43147(2)
0.15	-0.43322	-0.43369	-0.43396	-0.43530(2)
0.20	-0.43661	-0.43746	-0.43797	-0.44064(2)
0.25	-0.44055	-0.44192	-0.44271	-0.44727(2)

TABLE II: DMRG ground state energies for 12×12 lattices for second order DMRG compared with QMC for $ms_1 = ms_2 = 16, 24$ and 32 .

case for all values of J_{\perp} studied. But the improvement is small. This is because as discussed above, the DMRG does not provide the full 1D spectrum. Only the states kept to form the reduced superblock are used in the perturbative expansion. When $ms_2 = 32$, this is merely 924 states i.e., a tiny fraction of the 2^{144} states which form the full Hilbert space of the 12×12 lattice. Another reason for this modest improvement is the fact that the DMRG energies are variational. The high lying energies which are used to generate second order terms are obtained with less accuracy than the states kept in the first order. Indeed, this does not mean that the matrix expansion presented above is not efficient. It has been used in the simple case of the Mathieu equation for which the full spectrum of unperturbed Hamiltonian is available²⁰. The convergence of the matrix method is quite impressive. Thus it seems that the best way to use the matrix Kato-Block expansion when the DMRG is used to obtain the unperturbed spectrum is to restrict oneself to the first order and keep ms_2 as large as possible. However, larger values of ms_2 are unpractical when four blocks are used to form the superblock in the second step. For this reason from now, only three blocks will be used to generate the superblock in the second step.

VI. FIRST ORDER RESULTS WITH THREE BLOCKS IN STEP 2

When three blocks are used, the superblock size in the second step is divided by ms_2 relative to the case of four blocks. This significantly reduces the amount of required CPU for a given value of ms_2 . But this is not without problems. It was noted that², when three blocks are used, the coupling between blocks may incorrectly sets in leading to a poor performance of the method even if the truncation errors are small. The remedy against this problem is to target more than one state so that the interblock mixture is performed correctly. However, targeting many superblock states lower the accuracy on the ground state. For this reason, only the ground state was targeted. The truncation errors were in general smaller than 10^{-8} for ms_2 varying from 16 to 96 for different lattice size. But as said above, this does not give any indication about the accuracy of the second step of the

J_{\perp}	$ms_2 = 16$	$ms_2 = 32$	$ms_2 = 64$	QMC
0.00	-0.42187	-0.42187	-0.42187	-0.42186(2)
0.05	-0.42239	-0.42244	-0.42247	-0.42246(2)
0.10	-0.42402	-0.42421	-0.42439	-0.42444(2)
0.15	-0.42670	-0.42722	-0.42762	-0.42771(2)
0.20	-0.43032	-0.43144	-0.43219	-0.43239(2)
0.25	-0.43470	-0.43673	-0.43799	-0.43843(2)

TABLE III: DMRG ground state energies for 8×9 lattices for $ms_1 = 16$, and $ms_2 = 16, 32$, and 64 versus QMC.

J_{\perp}	$ms_2 = 32$	$ms_2 = 64$	$ms_2 = 80$	QMC
0.00	-0.42851	-0.42851	-0.42851	-0.42850(1)
0.05	-0.42910	-0.42918	-0.42919	-0.42922(1)
0.10	-0.43094	-0.43124	-0.43131	-0.43150(1)
0.15	-0.43396	-0.43468	-0.43483	-0.43537(1)
0.20	-0.43796	-0.43928	-0.43956	-0.44075(1)
0.25	-0.44268	-0.44476	-0.44521	-0.44744(1)

TABLE IV: DMRG ground state energies for 12×13 lattices for $ms_1 = ms_2 = 32, ms_2 = 64$ and $ms_2 = 80$ ($ms_1 = 64$ for both) versus QMC.

method. The QMC results are thus taken as the reference to gauge the DMRG results.

A. Ground-state energies

For small sizes and weak couplings, the differences between the DMRG and QMC ground state energies are very small. For instance for the 8×9 lattice shown in Table(III), for $J_{\perp} = 0.05$, the difference between the two methods is only 0.00016 for $ms_2 = 16$. The two results are within QMC error when ms_2 is increased to 64. As expected, increasing the coupling tends to decrease the accuracy because the ratio $\delta E(L)/J_{\perp}$ is reduced. Increasing the lattice size has the same effect on this ratio because $\delta E(L)$ is smaller for larger lattices for a fixed ms_2 (Table(III, IV, V)). One may note that by keeping a larger number of states than in the case of four blocks, the accuracy has increased in all cases.

$L \times L + 1$	DMRG	QMC
8×9	-0.42440	-0.42444(2)
12×13	-0.43124	-0.43150(2)
16×17	-0.43481	-0.43529(1)

TABLE V: DMRG ground state energies for various lattices for $ms_2 = 80$ and $J_{\perp} = 0.1$.

l	DMRG (l)	QMC (l)	DMRG (t)	QMC (t)
1	-0.14595	-0.14931(1)	-0.02047	-0.02209(1)
2	0.06072	0.05904(1)	0.00561	0.00525(1)
3	-0.04799	-0.05173(1)	-0.00191	-0.00164
4	0.03340	0.03537(1)	0.00066	0.00055
5			-0.00023	-0.00019

TABLE VI: DMRG versus QMC longitudinal (l) $\bar{C}_{\parallel}(7, 7, r)$ and transverse $\bar{C}_{\perp}(7, 7, r)$ spin-spin correlations for a 12×13 lattice for $J_{\perp} = 0.1$, $J_d = 0$.

B. Ground-state correlation functions

It is not possible to keep track of all spin-spin correlations when large systems are studied because of CPU and memory limitations. The behavior of spin-spin correlations is thus studied along one chain in the direction parallel to the chains and one chain in the direction perpendicular to the chains. These correlation functions are respectively given below:

$$C_{\parallel}(i, l, r) = \frac{1}{3} \langle \mathbf{S}_{i,l} \cdot \mathbf{S}_{i+r,l} \rangle, \quad (27)$$

$$C_{\perp}(i, l, r) = \frac{1}{3} \langle \mathbf{S}_{i,l} \cdot \mathbf{S}_{i,l+r} \rangle \quad (28)$$

It is particularly difficult to obtain the large r behavior of the correlation functions because of a number of factors that complicate such an analysis. At the level of a single chain, the long distance behavior of $C(i, r)$ is already complicated by logarithmic corrections. Although highly accurate data can be obtained in 1D from QMC³⁴ or DMRG³⁵, the two studies disagree on the exact form of the logarithmic corrections. Furthermore when open boundary conditions (OBC) are used instead of periodic, the spin-spin correlation functions show strong odd-even alternations^{2,29}. This is because the ground state may be regarded as a resonant state between a state with strong bonds on even links and weak bonds on odd links, and a state with weak bonds on even links and strong bonds on odd links. Another difficulty with OBC is that the translational invariance of the chain is broken, and the value of $C_{\parallel}(i, l, r)$ depends on the position of the site chosen as the origin on the lattice. It was shown²⁹ that the closer the origin is to the edge of the lattice, the higher are the spurious effects introduced by the OBC. All these facts render the direct detection of long range order in the transverse direction, for which the spin-spin correlations are very small, impossible to achieve with the present calculation for which the magnitude of $C_{\perp}(i, l, r)$ for large r is close to the accuracy on the eigenvalues during each iteration. An alternative way is to look at the $C_{\parallel}(i, l, r)$, because the existence of long range order in the longitudinal direction is an indication that the order is two-dimensional.

In order to observe the correct long-range behavior, one must first reduce the influence of the spurious effects

l	DMRG (l)	QMC (l)	DMRG (t)	QMC (t)
1	-0.14640	-0.14619(1)	-0.02116	-0.02533(1)
2	0.06059	0.06130(1)	0.00726	0.00854(1)
3	-0.04875	-0.04988(1)	-0.00320	-0.00399
4	0.03422	0.03537(1)	0.00147	0.00201
5	-0.02866	-0.02990(1)	-0.00078	-0.00105
6	0.02251	0.02363(1)	0.00030	0.00056
7			-0.00013	-0.00030
8			0.00006	0.00015

TABLE VII: DMRG versus QMC longitudinal (l) $\bar{C}_{\parallel}(9, 9, r)$ and transverse $\bar{C}_{\perp}(9, 9, r)$ spin-spin correlations for a 16×17 lattice for $J_{\perp} = 0.1$, $J_d = 0$.

generated by the application of the OBC. Furthermore to simplify the analysis, the eventual logarithmic corrections will not be considered here. In order to avoid the odd-even alternation, $C_{\parallel}(i, l, r)$ and $C_{\perp}(i, l, r)$ were averaged in the period of these alternations. This was done by computing $\langle \mathbf{S}_{i,l} \mathbf{S}_{i+r,l} \rangle$ at two different origins. The spin \mathbf{S}_{il} is taken as the origin of a strong link or as the origin of a weak link. The actual correlation function is then

$$\bar{C}_{\parallel}(i, l, r) = 0.5(C_{\parallel}(i, l, r) + C_{\parallel}(i+1, l, r)). \quad (29)$$

And for $C_{\perp}(i, l, r)$,

$$\bar{C}_{\perp}(i, l, r) = 0.5(C_{\perp}(i, l, r) + C_{\perp}(i, l-1, r)). \quad (30)$$

The averaged correlations $\bar{C}_{\parallel}(i, l, r)$ and $\bar{C}_{\perp}(i, l, r)$ are shown in Tables VI, VII and VIII for, respectively, 12×13 , 16×17 and 32×33 lattices. The origins (i, l) of the correlation functions were chosen at the middle of the chain in order to minimize the end effects. (i, l) was equal to $(7, 7)$, $(9, 9)$ and $(17, 17)$ respectively for the 12×13 , 16×17 and 32×33 lattices. For the 16×17 lattice, $ms_1 = 128$ states were kept during the first DMRG step and $ms_2 = 64$ states were kept during the second DMRG step. The comparison with QMC is quite good in the longitudinal direction but less good in the transverse direction when the lattice size gets large. For the 32×33 lattice, ms_1 and ms_2 were respectively increased to 160 and 80. As for the case of the 16×17 lattice the agreement was quite good for $\bar{C}_{\parallel}(i, l, r)$ and less good for $\bar{C}_{\perp}(i, l, r)$. The reasons for the differences are not easy to analyze. Although very small truncation errors p_m (for instance, $p_m < 1 \times 10^{-7}$ for $ms_1 = 128$ and $ms_2 = 64$) are obtained in the DMRG, there is no obvious relation between these truncation errors and the errors on the measurements. Furthermore, the effects of higher order terms in the perturbation series have not been analyzed for the case of three blocks. Since more states are kept when three blocks are used, the contribution of second order terms is likely larger than the one found above for four blocks.

l	DMRG (l)	QMC (l)	DMRG (t)	QMC (t)
1	-0.14694	-0.14636(3)	-0.01846	-0.02952(2)
2	0.06042	0.06151(3)	0.00969	0.01465(2)
3	-0.04908	-0.05066(2)	-0.00623	-0.01057(3)
4	0.03402	0.03640(2)	0.00416	0.00821(1)
5	-0.02949	-0.03229(3)	-0.00281	-0.00662(1)
6	0.02366	0.02682(3)	0.00190	0.00545(1)
7	-0.02108	-0.02450(2)	-0.00128	-0.00453(2)
8	0.01820	0.02163(3)	0.00086	0.00379(2)
9	-0.01643	-0.01990(2)	-0.00059	-0.00321(2)
10	0.01474	0.01806(2)	0.00040	0.00270(2)
11	-0.01327	-0.01646(2)	-0.00028	-0.00228(2)
12	0.01202	0.01508(2)	0.00018	0.00194(2)
13	-0.01045	-0.01309(1)	-0.00012	-0.00164(2)
14	0.00914	0.01164(2)	0.00008	0.00137(2)
15			-0.00005	-0.00115(1)
16			0.00003	0.00088(1)

TABLE VIII: DMRG versus QMC longitudinal (l) $\bar{C}_{\parallel}(17, 17, r)$, and transverse (t) $\bar{C}_{\perp}(17, 17, r)$ spin-spin correlations for a 32×33 lattice for $J_{\perp} = 0.1$, $J_d = 0$.

VII. GROUND-STATE PROPERTIES IN PRESENCE OF FRUSTRATION

The DMRG method has shown an overall good agreement with QMC for weak couplings and not too large sizes. The method is well controlled and can systematically be improved by increasing ms_1 and ms_2 . The advantage of the DMRG over QMC is that it is very flexible and can be applied to frustrated systems. A situation where the QMC is known to fail. In this section a diagonal J_d exchange coupling is included. It has the effect of introducing a competition between interchain AFM correlations along the rows and AFM correlations along the diagonals.

A. Ground-state energies

Although the result on the ground state energy can not provide information about a possible long-range order, it can be helpful to see if the perturbation is relevant or not. Fig. 5 shows the binding energy per chain $E_B = E_0(L) - E_0(L \times (L+1)) / (L+1)$, where $E_0(L)$ is the ground state energy for a single chain and $E_0(L \times (L+1))$ is the ground state energy for an $L \times (L+1)$ lattice. J_{\perp} is set to 0.1. E_B first decreases as J_d/J_{\perp} is increased. It reaches a minimum at $J_d \approx 0.5J_{\perp}$. At the minimum point, the binding energy nearly vanishes, $E_B \approx 0.0015$ which is roughly two orders of magnitude smaller than its value for $J_d = 0$. As J_d/J_{\perp} is further increased, E_B starts increasing sharply. This behavior suggests the existence of three regimes for the action of small perturbations on the single chain, two stable phases separated by a transition region. The first regime, which occurs when $J_d \lesssim 0.5J_{\perp}$, is a Néel state as is already known from QMC studies¹⁴. This will be confirmed below by the

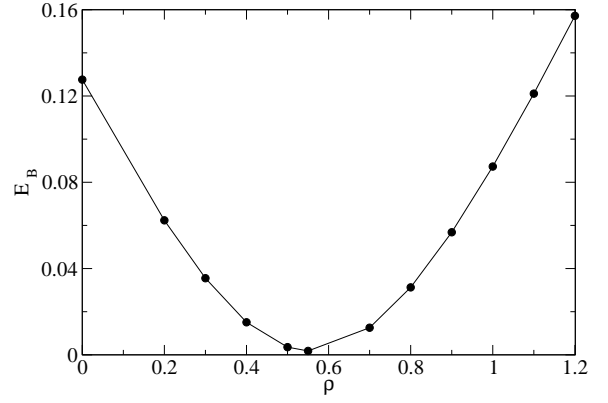


FIG. 5: The binding energy E_B with respect to single chain for a 32×33 lattice as a function of $\rho = J_d/J_{\perp}$, $J_{\perp} = 0.1$.

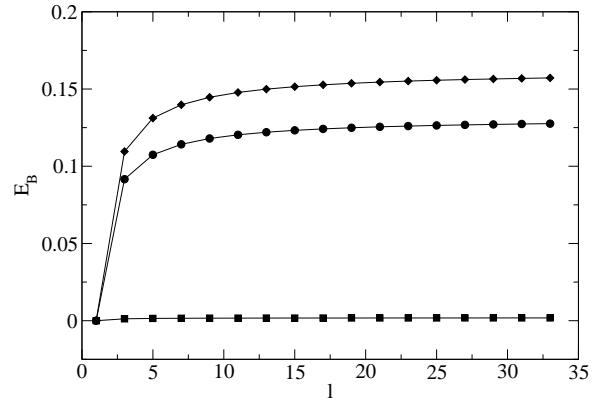


FIG. 6: The binding energy E_B with respect to single chain for a $32 \times l$ lattice as a function of l for $J_d/J_{\perp} = 0$ (circles), $J_d/J_{\perp} = 0.5$ (squares), $J_d/J_{\perp} = 1.2$ (diamonds), $J_{\perp} = 0.1$.

analysis of the DMRG correlation functions. The second regime is when $J_d \approx 0.5J_{\perp}$. The perturbation seems to be irrelevant, J_{\perp} and J_d cancel each other so that there is almost no gain in energy by applying the two perturbations simultaneously. In the third regime, when $J_d \gtrsim 0.5J_{\perp}$, the ground state is also magnetic with a collinear order, an alternate arrangement of transverse up and down ferromagnetic chains (see Fig. 1).

The above analysis is further supported by observing the evolution of the binding energy $E_B(L \times l)$ as a function of the number of chains in the lattice (Fig. 6). It clearly shows that when $J_d \approx 0.5J_{\perp}$, the binding energy is nearly independent of the number of chains and remains very close to that of the single chain. Hence it seems that at the point $J_d \approx 0.5J_{\perp}$, the ground state is made of independent chains as for $J_{\perp} = J_d = 0$. This behavior is analogous to the domino model studied by Villain and coworkers³⁷, where a disordered ground state, made of independent chains for a particular value of the transverse coupling, was found.

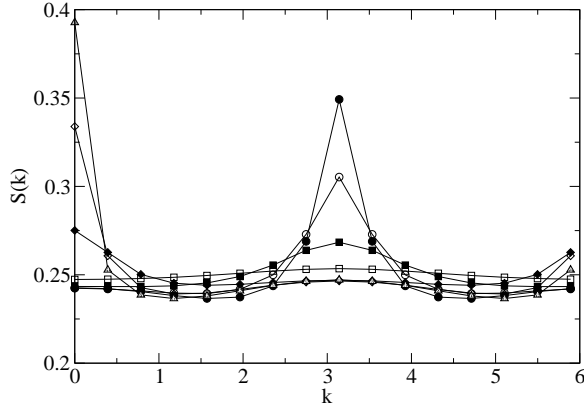


FIG. 7: The ground state transverse structure factor for a 32×33 lattice for $J_d/J_\perp = 0$ (filled circles), 0.2 (open circles), 0.4 (filled squares), 0.55 (open squares), 0.8 (filled diamonds), 1.0 (open diamonds), 1.2 (open triangles).

B. Ground-state correlation functions

The behavior of the correlation functions is consistent with the existence of the three regimes found for the ground state energy. As expected, spin-spin correlations along the chains remain antiferromagnetic. The change of regimes will be detected by analyzing spin-spin correlations along the transverse direction. Fig. 7 shows the transverse magnetic structure factor $S_\perp(k_\perp)$,

$$S_\perp(k_\perp) = \sum_{k_\perp=1}^{L/2} \bar{C}_\perp(17, 17, r) \cos k_\perp r \quad (31)$$

where k_\perp is a wave number in the transverse direction. It also shows the three regimes discussed above. When $J_d \lesssim 0.5J_\perp$, $S_\perp(k_\perp)$ has a maximum at $k_\perp = \pi$. The spin-spin correlations along the transverse direction are AFM as for the longitudinal direction. For $J_d \approx 0.5J_\perp$, S_\perp is structureless, a fact which is consistent with disconnected chains. When $J_d \gtrsim 0.5J_\perp$, S_\perp has a maximum at $k_\perp = 0$, and the correlations in the transverse direction are now ferromagnetic. This is the collinear magnetic state shown in Fig. 1.

The bond-strength $\bar{C}_\perp(17, 17, 1)$, computed in a 32×33 lattice is shown in Fig. 8. It also shows that the chains seem to be disconnected when $J_d \approx 0.5J_\perp$. Starting from $J_d = 0$, for which $\bar{C}_\perp(17, 17, 1) = -0.01846$, its absolute value first slowly decreases. Then, when J_d is in the vicinity of J_{dC} , the absolute value of $\bar{C}_\perp(17, 17, 1)$ sharply decreases and become very small; $\bar{C}_\perp(17, 17, 1) = -0.000799$ when $J_d = 0.5J_\perp$. As soon as J_d exceeds J_{dC} , $\bar{C}_\perp(17, 17, 1)$ becomes ferromagnetic and starts to increase sharply. It later saturates when one is far enough from the critical point.

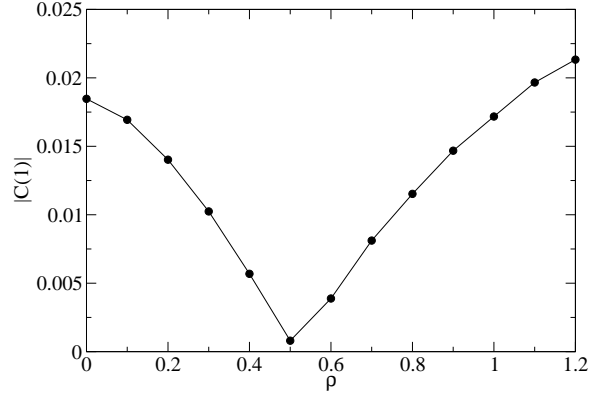


FIG. 8: The bond-strength $C(1) = \bar{C}_\perp(17, 17, 1)$ as a function of $\rho = J_d/J_\perp$, $J_\perp = 0.1$.

VIII. LONG-RANGE ORDER IN THE GROUND STATE

The analysis made in the preceding section indicates regions of dominant Néel or collinear spin-spin correlations or of a possibly disordered ground state at the transition point. But it does not tell if long range order is truly established. For this, it is necessary to look at the long-range behavior of the correlation functions.

The spurious effects due to the breaking of the translational symmetry, a consequence of the OBC, may be reduced by using a filter which smooths the action of the sites near the edges. In the results shown below in Fig 9, 10, 11, this was done as follows: $\bar{C}_\parallel(i, l, r)$ was first examined for a single chain for which the long distance behavior is known. Roughly, $\bar{C}_\parallel(i, l, r) \propto 1/r$ if logarithmic corrections are neglected. It was found that if the origin is taken at the middle of the chain, the $1/r$ behavior is roughly satisfied for $d \lesssim r \lesssim L/2 - d$ with $d \approx 8$. The second inequality is due to edge effects. As a consequence, relatively large values of L are necessary in order to observe the long range behavior, and lattices of up to 64×65 were studied. The problem with such large lattices is that the energy width $\delta E(L)$ shrinks with increasing L and the condition $\Delta_\sigma(L) \simeq J_{\perp,d} \ll \delta E(L)$ may not be fulfilled. For $L = 64$, $ms_1 = 192$ and $ms_2 = 80$ states were kept. For these values, $\delta E(L = 64) \approx 0.5$, which means $\delta E(L = 64)/J_{\perp,d} \approx 5$ provided that $J_{\perp,d} \lesssim 0.16$.

The first question which needs to be addressed is to know whether the DMRG can detect an eventual long range order. Comparisons with QMC for $L = 32$ show that, the DMRG correlation in the transverse direction decays faster. This effect is expected to be larger on longer chains. But, despite this shortcoming of the method, one can still detect possible occurrence of long range order. If one considers the central chain in the 2D lattice, $\bar{C}_\parallel(L/2+1, L/2+1, r)$ is modified from that of an isolated chain because of the effective magnetic field created on it by the rest of lattice. Although this effective field is somewhat underevaluated by the DMRG because

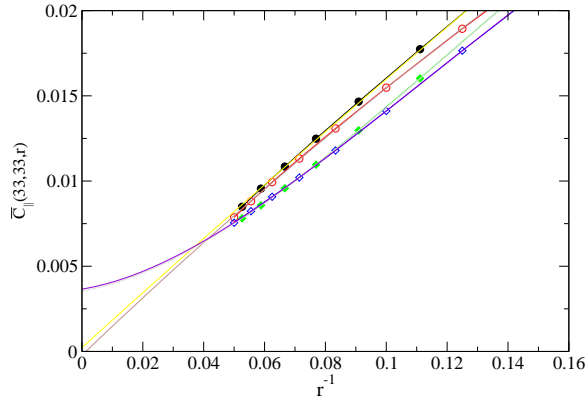


FIG. 9: The ground state correlation function $\bar{C}_{\parallel}(33,33,r)$ for the 64×65 lattice for $J_{\perp} = 0$ (circles) and $J_{\perp} = 0.16$ (squares). $J_d = 0$ in both cases. The filled and open symbols correspond to odd and even distances respectively.

the transverse correlations are underevaluated, it can still be strong enough to lead to an ordered phase. This interpretation is related to the chain mean-field approach³⁶; the essential point is that, here, no assumption about long-range order is made *a priori*. From this, one can see that if the DMRG method leads to a finite order parameter, it is necessarily genuine. Fig. 9 compares for the correlation function $\bar{C}_{\parallel}(33,33,r)$ for $J_{\perp} = 0$, $J_d = 0$ with $J_{\perp} = 0.16$, $J_d = 0$. In the first case when both transverse couplings are absent, $\bar{C}_{\parallel}(33,33,r) \propto 1/r$. The DMRG data still show an odd-even alternation, so fits must be performed for odd and even distances separately. The best least square fits to the data gave $\bar{C}_{\parallel}(33,33,r \rightarrow \infty) \approx 0.0001$. This is consistent with an absence of a long-range order for an isolated chain. But in the case $J_{\perp} = 0.16$ and $J_d = 0$, a fit to the data shows that $\bar{C}_{\parallel}(33,33,r)$ tends to $\bar{C}_{\parallel}(33,33,r \rightarrow \infty) \approx 0.0036$. The existence of long-range Néel order for $J_{\perp} = 0.16$ is consistent with previous studies^{12,14}. Adding J_{\perp} alone seems to lead to long-range order. This has been recently shown in Ref.¹⁴ where values of J_{\perp} down to 0.02 were investigated. It is of course impossible to show from a numerical investigation whether any small value of J_{\perp} will lead to an ordered state or there may be a disordered state for very small values of J_{\perp} . In view of current numerical results, the former hypothesis is more convincing.

The above discussion suggests that a frustration J_d must be added in order to thwart the Néel state which results from the action of J_{\perp} . J_{\perp} will now be set to 0.16 and J_d varied. For $J_d = 0.08$, the value at which the analysis of smaller chains suggested that the ground state is made of disconnected chains, $\bar{C}_{\parallel}(33,33,r)$ is compared to the same quantity for a single chain in Fig. 10. Fits to the data show that the behavior of $\bar{C}_{\parallel}(33,33,r)$ is quite similar to that of a single chain. Clearly, for these values of the transverse couplings there is no long-range order in the ground state, and $\bar{C}_{\parallel}(33,33,r)$ seems to indicate that the ground state is made of a set of independent chains. It is important to emphasize that this

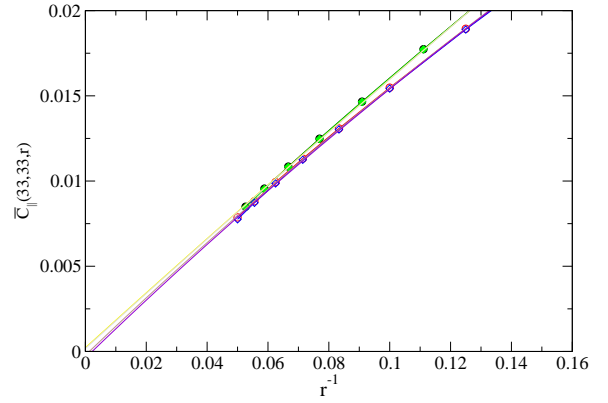


FIG. 10: The ground state correlation function $\bar{C}_{\parallel}(33,33,r)$ for the 64×65 lattice for $J_{\perp} = 0$, $J_d = 0$ (circles) and $J_{\perp} = 0.16$, $J_d = 0.08$ (squares). The filled and open symbols correspond to odd and even distances respectively.

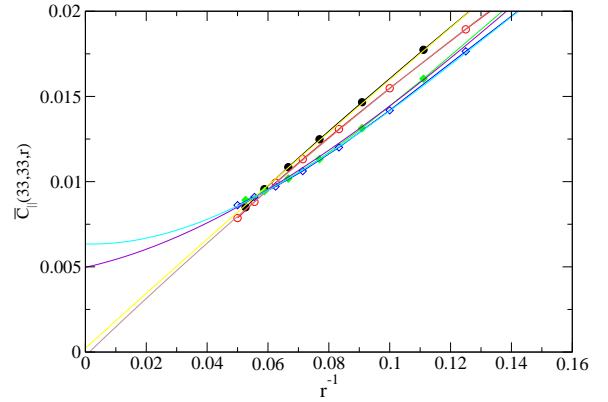


FIG. 11: The ground state correlation function $\bar{C}_{\parallel}(33,33,r)$ for the 64×65 lattice for $J_{\perp} = 0$, $J_d = 0$ (circles) and $J_{\perp} = 0.16$, $J_d = 0.16$ (squares). The filled and open symbols correspond to odd and even distances respectively.

result does not mean that the finite temperature effects are also trivial. The present situation could be similar to the so-called domino model first introduced by Andre³⁸ and later studied by Villain and coworkers³⁷ or to the crossed-chains quantum spin models²⁵. In the domino model, it was found that the ground state was made of disconnected chains but there was a long-range order at finite temperature. Indeed, the Mermin-Wagner theorem prohibits long-range order at finite temperatures for the 2D Heisenberg model. The finite temperature behavior in this case will thus be different.

The disconnected chain ground state is in contradiction with a recent study by Nersisyan and Tsvelik¹⁵. These authors argued, using bosonization, that when $J_d/J_{\perp} = 0.5$, only the staggered part of the interchain part of the Hamiltonian vanishes. There remains a uniform part which is relevant and leads to two-dimensional spin liquid with a spin gap, $\Delta_{\sigma} \propto \exp(-\frac{\pi v_{\sigma}}{2J_{\perp}})$, where v_{σ} is the spin velocity. The low energy excitations are argued to be unconfined spinons. The apparent contra-

diction between this conclusion and the numerical data above could be that the binding energies of the 2D spin liquid are very small, indeed $J_{\perp} = 0.1$ corresponds to $\Delta_{\sigma} \approx 1.0 \times 10^{-11}$. Such a small energy can obviously not be detected by a numerical method. A way to avoid this small energy scale is to raise J_{\perp} . This possibility is currently being investigated.

Finally, the collinear magnetic long range order is also confirmed by the analysis of $\bar{C}_{\parallel}(33, 33, r)$. In Fig. 11, it is shown that for $J_d = 0.1$, $\bar{C}_{\parallel}(33, 33, r)$ converges even faster than for the Néel state above. The value of the extrapolated correlation is $\bar{C}_{\parallel}(33, 33, r \rightarrow \infty) \approx 0.0056$.

IX. CONCLUSIONS

In this paper, a new renormalization group method for weakly coupled chains was presented. It is based on solving numerically the model Hamiltonian in two 1D steps using the DMRG. During the first step, a low energy Hamiltonian for a single chain is obtained using the 1D DMRG. The original problem is then formulated as a perturbative expansion around the DMRG low energy Hamiltonian obtained during the first step. This perturbative expansion is a 1D problem which can also be solved by the DMRG.

The first and second order approximations were studied for weakly coupled Heisenberg chains with and without frustration. The results were compared to the QMC and showed good agreement for small systems and small transverse couplings. It was shown that, starting from

the disordered 1D chain, the method can predict long-range order when it exists, a test generally failed by conventional perturbative methods. Calculations performed in the presence of frustration indicate an absence of a genuinely 2D spin liquid state. Instead, the frustration drives the Néel ground state to a collinear magnetic state. At the transition point, both ground-state energy and spin-spin correlation functions show a disordered ground state. The precise nature of this disordered ground state is currently under investigation.

The above results are very encouraging and indicate that the DMRG may become a very useful tool for the study of highly anisotropic 2D systems in the future. The method is only in its early stages, and some important improvements of the method are currently underway. These are the investigation of the role of cluster corrections, i.e., the starting point in the first step will be two-leg or three-leg ladders instead of a single chain; the use of exact diagonalization during the first step instead of DMRG. These improvements are likely to lead to better results for spin-spin correlations in the transverse direction. Extensions of the method to thermodynamic spin systems or fermionic models will also be made in the near future.

Acknowledgments

I am very grateful to A. Sandvik for sharing his QMC data and for numerous helpful exchanges during the course of this work. I wish to thank J.V. Alvarez for useful discussions. I also thank J.W. Allen and P. McRobbie for reading the manuscript.

-
- ¹ S. Moukouri and L.G. Caron, Phys. Rev. **B 67**, 092405 (2003).
 - ² S.R. White, Phys. Rev. Lett. **69**, 2863 (1992). Phys. Rev. **B 48**, 10 345 (1993).
 - ³ 'Density-Matrix Renormalization', Ed. By I. Peschel, X. Wang, M. Kaulke and K. Hallberg, Springer (1998)
 - ⁴ P.W. Anderson, Science **235**, 1169 (1987).
 - ⁵ P. Fazekas and P.W. Anderson, Philos. Mag. **30**, 423 (1974).
 - ⁶ P. Chandra and B. Douçot, Phys. Rev. **B 38**, 9335 (1988).
 - ⁷ E. Dagotto and A. Moreo, Phys. Rev. Lett. **63**, 2148 (1989).
 - ⁸ P. Chandra, P. Coleman and A.I. Larkin, Phys. Rev. Lett. **64**, 88 (1990).
 - ⁹ L. Capriotti and S. Sorella, Phys. Rev. Lett. **84**, 3173 (2000).
 - ¹⁰ N. Read and S. Sachdev, Phys. Rev. Lett. **66**, 1773 (1992).
 - ¹¹ A. Parola, S. Sorella and Q.F. Zhong, Phys. Rev. Lett. **71**, 4393 (1993).
 - ¹² I. Affleck, M.P. Gelfand and R.R.P. Singh, J. Phys. **A 27** 7313 (1994); Erratum *ibid.* **A 28**, 1787 (1995).
 - ¹³ H. Rosner *et al.*, Phys. Rev. **56**, 3402 (1997).
 - ¹⁴ A.W. Sandvik, Phys. Rev. Lett. **83**, 3069 (1999).
 - ¹⁵ A.A. Nersisyan and A.M. Tsvelik, cond-mat/0206483.
 - ¹⁶ S. K. Satija *et al.*, Phys. Rev. **B 21**, 2001 (1980).
 - ¹⁷ A. Keren *et al.*, Phys. Rev. **48**, 12926 (1993).
 - ¹⁸ D. A. Tennant *et al.*, Phys. Rev. **B 52**, 13381 (1995).
 - ¹⁹ R. Coldea *et al.* Phys. Rev. Lett **86**, 1335 (2001).
 - ²⁰ S. Moukouri physics/0312011.
 - ²¹ T. Kato, Prog. Teor. Phys. **4**, 514 (1949); **5**, 95 (1950).
 - ²² C. Bloch, Nucl. Phys. **6**, 329 (1958).
 - ²³ A. Messiah 'Quantum Mechanics', Ed. Dover, p. 685-720 (1999).
 - ²⁴ J.E. Hirsch and G.F. Mazenko, Phys. Rev. **B 19**, 2656 (1979).
 - ²⁵ O.A. Starykh, R.R.P. Singh and G.C. Levine, Phys. Rev. Lett. **88**, 167203 (2002).
 - ²⁶ R. Mukhopadhyay, *et al.* Phys. Rev. **B 64**, 045120 (2001).
 - ²⁷ S. Moukouri and L.G. Caron, Phys. Rev. Lett. **77**, 4640 (1996).
 - ²⁸ T. Sakai and M. Takahashi, J. Phys. Soc. Jpn. **58**, 3131 (1989).
 - ²⁹ L.G. Caron and C. Bourbonnais, Phys. Rev. **66**, 045101 (2002).
 - ³⁰ S.R. White and R.M. Noack, Phys. Rev. Lett. **68**, 3487 (1992).
 - ³¹ S.D. Drell, M. Weinstein and S. Yankielowicz, Phys. Rev. **D 14**, 487 (1976).
 - ³² R. Jullien, P. Pfeuty, J.N. Fields and S. Doniach, Phys. Rev. **B 18**, 3568 (1978).

- ³³ A.W. Sandvik and J. Kurkijärvi, Phys. Rev. **B** **43**, 5950 (1991); A.W. Sandvik, Phys. Rev. **B** **59**, 14157 (1999).
- ³⁴ A.W. Sandvik and D.J. Scalapino, Phys. Rev. **47**, 12333 (1993).
- ³⁵ K. Hallberg, P. Horsch and G. Martinez, Phys. Rev. **52**, 719 (1995).
- ³⁶ D.J. Scalapino, Y. Imry, and P. Pincus, Phys. Rev. **B** **11**, 2042 (1975).
- ³⁷ J. Villain, R. Bidaux, J.-P. Carton and R. Conte, J. Physique **41**, 1263 (1980).
- ³⁸ G. André, R. Bidaux, R. Conte and L. de Seze, J. Physique **40**, 479 (1979).